Single channel approach for filtering EEG signals strongly contaminated with facial EMG

Gustavo Moreira da Silva
Universidade Federal de Uberlandia
Carlos Magno Medeiros Queiroz
UFU: Universidade Federal de Uberlandia
Steffen Walter (steffen.walter@uni-ulm.de)
University Hospital Ulm: Universitatsklinikum Ulm https://orcid.org/0000-0001-7165-3541
Luciano Brink Peres
Universidade Federal de Uberlandia
Luiza Maire David Luiz
Universidade Federal de Uberlandia
Samila Carolina Costa
Universidade Federal de Uberlandia
Adriano Alves Pereira
Universidade Federal de Uberlandia
Marcus Fraga Vieira
Federal University of Goias: Universidade Federal de Goias
Adriano de Oliveira Andrade
Universidade Federal de Uberlandia

Research

Keywords: EEG filtering, facial EMG noise, EMDRLS, Empirical Mode Decomposition, Adaptative Filtering, Recursive Least Squares filtering

Posted Date: October 6th, 2020

DOI: https://doi.org/10.21203/rs.3.rs-85029/v1

Single channel approach for filtering EEG signals strongly contaminated with facial EMG

Gustavo Moreira da Silva[1¶], Carlos Magno Medeiros Queiroz[1§], Steffen Walter[2¥*], Luciano Brink Peres[1§], Luiza Maire David Luiz[1§], Samila Carolina Costa[1§], Adriano Alves Pereira [1¥], Marcus Fraga Vieira [3¥], Adriano de Oliveira Andrade[1£]

[1] Centre for Innovation and Technology Assessment in Health, Federal University of Uberlândia, Uberlândia, Brazil.

[2] Department of Medical Psychology, Clinic of Psychosomatic Medicine and Psychotherapy, University Hospital Ulm, Ulm, Germany

[3] Bioengineering and Biomechanics Laboratory, Federal University of Goiás, Goiânia, Brazil.

* Corresponding author

E-mail: steffen.walter@uni-ulm.de

Abstract

Background

Eliminating facial electromyography (EMG) from the electroencephalogram (EEG) is essential for the accuracy of applications such as brain computer interfaces (BCIs) and quantification of brain functionality. Although it is possible to find several studies that address EEG filtering, there is lack of researches that improve the filtering of EEG strongly corrupted by EMG signals with single-channel approaches, which are necessary in situations in which the number of available channels is reduced for the application of filtering methods based on multichannel techniques. In this context, this research proposes an EEG denoising method for filtering EMG from the masseter and frontal. This method, so-called EMDRLS, combines the use of Empirical Mode Decomposition (EMD) and a Recursive Least Square (RLS) filter to attenuate facial EMG noise from EEG. The results were compared with those obtained from Wavelet, EMD, Wiener and Wavelet-RLS (WRLS) filters. Besides the visual inspection of the resultant waveform of filtered signals, the following objective metrics were employed to contrast the performance of the filtering methods: (i) the signal-noise ratio (SNR) of the contaminated signal, (ii) the root mean square error (RMSE) between the power spectrum of artifact free and filtered EEG epochs, (iii) the spectral preservation of brain rhythms (i.e., delta, theta, alpha, beta, and gamma rhythms) of filtered signals.

Results

The EMDRLS method yielded filtered EEG signals with SNR varying from 0 to 10 dB for EEG signals with SNR below -10dB. The Spearman's correlation coefficient estimated between the SNR of filtered and corrupted signals was below 0.04, suggesting, in the evaluated conditions, the independence of the EMDRLS filtering performance to the SNR of noisy signals. The technique also improved the RMSE between the power spectrum of artifact free and filtered EEG epochs by a factor of 27 (from 5.429 to 0.197) in the most corrupted EEG channels with the masseter muscle contraction. The Kruskal-Wallis test and the Tukey-Kramer post-hoc test ($p < 0.05$) confirmed the preservation of all brain rhythms given by EEG signals filtered with the EMDRLS method.

Conclusions

The results showed that the single-channel EMDRLS method can be applied to highly contaminated EEG signals by facial EMG signal with performance superior to that of the compared methods. The method can be applied for the offline filtering of EEG signals contaminated by facial EMG.

Keywords: EEG filtering, facial EMG noise, EMDRLS, Empirical Mode Decomposition, Adaptative Filtering, Recursive Least Squares filtering.

Background

Electroencephalography is a technique used to record the activity on the scalp of measured cerebral cortex neuronal populations. It is derived from a high temporal resolution, non-invasive macroscopic process and is a low-cost method compared to a functional neuroimaging test [1]. The electroencephalogram (EEG) is widely used in a variety of clinical and commercial applications, including cognitive neuroscience, brain-skill quantification, pathological diagnosis, biometrics and Brain-Computer Interfaces (BCIs) [2–5].

The system for measuring EEG amplifies the tiny disturbances of the electrical potentials of the electrodes positioned on the scalp, which is anatomically separated from the signal-generating sources by the meninges, skull bones, and scalp. Thus, the synaptic potentials which usually have low amplitudes, in the order of millivolts, are strongly attenuated by these anatomical structures, reducing the amplitude of the signals recorded at the scalp [6]. Due to this low amplitude, which typically does not exceed 100 μV, the EEG signal is highly susceptible to artifacts [7].

These artifacts are usually caused by electromagnetic fields generated by nearby electronic devices and the power grid. In addition, artifacts can be produced by other sources of electrophysiological signals (e.g., muscular and heart activity or eye movement) [8,9]. This contamination decreases the performance of applications such as BCI and diagnosis of pathological disfunctions, since the amplitude of the artifact will typically be several orders of magnitude greater than the EEG amplitude [10,11].

In this context, the characterization and attenuation of artifacts is relevant for the correct interpretation and use of EEG. Facial electromyographic (EMG) signals are a primary source of EEG contamination. The main challenge with respect to the attenuation of noise generated by the EMG signal lies in the fact that EMG emerges from the anatomically positioned muscles along the skull. Even weak muscular contractions can be detected throughout the scalp due to the phenomenon of conductive volume. In addition, the EMG signal overlaps the spectrum of the EEG signal in virtually all frequency bands [12].

To solve this problem, several EEG filtering methods are described in the literature. However, these methods have some limitations, mainly related to the inability to completely remove noise from the corrupted signal without the introduction of undesired distortions, and the need for a priori noise information for signal filtering. These limitations, associated with several features estimated from the EEG signal to suit the diversity of applications, motivate the search of methods to remove EEG artifacts [9,13–18].

Frequency selector filters, such as a linear Butterworth filter, are one of the main techniques described in the literature for the removal of physiological artifacts from EEG. However, the use of such filter class is only effective when the frequency range of the signal and noise are not overlapped [8].

The literature suggests the use of single-channel techniques for muscular artifact removal from EEG instead of multichannel techniques (e.g. Independent Component Analysis – ICA and Canonical Correlation Analysis – CCA). The following methods are commonly employed for this purpose: adaptive filtering [19,20]; wiener filtering [21,22], Bayesian filtering [23], Blind Source Separation (BSS) [24,25], wavelet transform (WT) [26,27], Empirical Mode Decomposition (EMD) [28,29] and the combination of these techniques (i.e., hybrid methods) [14,30–33].

An adaptive filter is required when fixed specifications are unknown. The most prevalent family of algorithms for removing EEG artifacts is based on the method of least squares [19,34]. Adaptive filters vary in time because their parameters are continuously changing to meet a performance requirement [35].

Wiener filtering is appropriate in situations in which the signal and noise spectrum are overlapping, although it requires an estimated, measured or reliable reference to operate [36]. Borowicz showed that the performance of the multichannel Wiener filter outperformed that of BSS for removal of EEG artifacts of various types, (i.e. those that were annotated as unwanted by the user) [37]. In addition, Ferdous and Ali [21] compared Wiener and Kalman filters, and again the Wiener filter was more effective for removing EEG artifacts. However, the Wiener filter was mainly applied to remove ocular artifacts, not including muscular artifacts with low SNR (i.e. lower than -10 dB).

Gao [38] employed an adaptive algorithm to remove ECG from EEG during sleep apnea records by means of Discrete Wavelet Transform (DWT). Iyer [39] compared DWT with an interactive ICA filter for subsequent detection of single-trial evoked potential. Krishnaveni [40] compared the JADE algorithm [41] with DWT for the removal of the electrooculogram contamination (EOG) from EEG.

Empirical Mode Decomposition (EMD) was successfully used for the removal of EEG artifacts in [13], [42] and also in conjunction with BSS methods [42,43]. A broad review of the application of EMD and its variations on EEG signal processing is given in [44].

Recent efforts have been focused on the combination of these algorithms for removing artifacts from the EEG. Hybrid methods are, therefore, considered the state of the art in EEG filtering because they use the advantages of different methods in two or more stages and have presented the best results in their applications

[8,9,14,15,30,45–47]. The main combinations of algorithms in different filtering stages are: (i) adaptive filtering with BSS-ICA; (ii) EMD with BSS; (iii) wavelet with BSS; (iv) adaptive filtering with EMD [45].

Mucarquer et al. [18] described a significant reduction in EMG contamination with the hybrid EEMD-CCA technique by employing an array of EMG channels to increase the number of observations for the blind source separation method. Somers et al. [48] addressed the removal of the EMG artifact and other EEG artifacts using Wiener's multi-channel technique. Although they presented favorable results, multichannel techniques have limitations because their efficiency is generally conditioned to the requirement of a larger number of channels, which may not be available in some applications. Saini et al. [49] reported an approach to remove EMG from EEG signals based on the use of single-channel variational mode decomposition. However, there was no analysis of the performance of the method on experimental EEG signals contaminated by EMG.

In general, single-channel techniques have been shown to be the most effective approaches for the removal of facial muscular artifacts from EEG, especially when a reference signal is known [50]. However, the main limitations of this class of noise removal technique is that its performance is low for signal-to-noise ratios below -10 dB [18,30,50], which is typical in EEG contaminated by facial EMG. This is important when there is a need to monitor brain activity during human computer interaction based on facial electromyography [51].

In order to contribute to the research of facial EMG removal from EEG, this study proposes an EEG filtering method for facial EMG removal that is independent of an external reference noise and is suitable for low SNR (e.g., less than -10 dB) signals. Thus, the hypothesis to be tested is that a single-channel EMG reference signal, estimated from EMD, in combination with a Recursive Least Squares (RLS) filter [35,52,53] improves the filtering of EEG strongly contaminated with facial EMG. The results of the proposed method, so-called EMDRLS, were compared with those obtained from traditional methods such as the wavelet transform, Wiener filtering, EMD and hybrid filtering. The experimental protocol adopted in this study is based on the practical need of assessing brain activity for motor learning quantification during the interaction with a myoelectric interface [51].

Results

Visual Inspection

Figure 1 presents a visual inspection of a typical EEG epoch from channel F7-F3 with EMG contamination from masseter muscular contraction. The hybrid techniques, EMDRLS and wRLS, successfully remove the EMG

contamination. However, the wRLS method alters the waveform of the noise-free region to a greater extent than EMDRLS method.

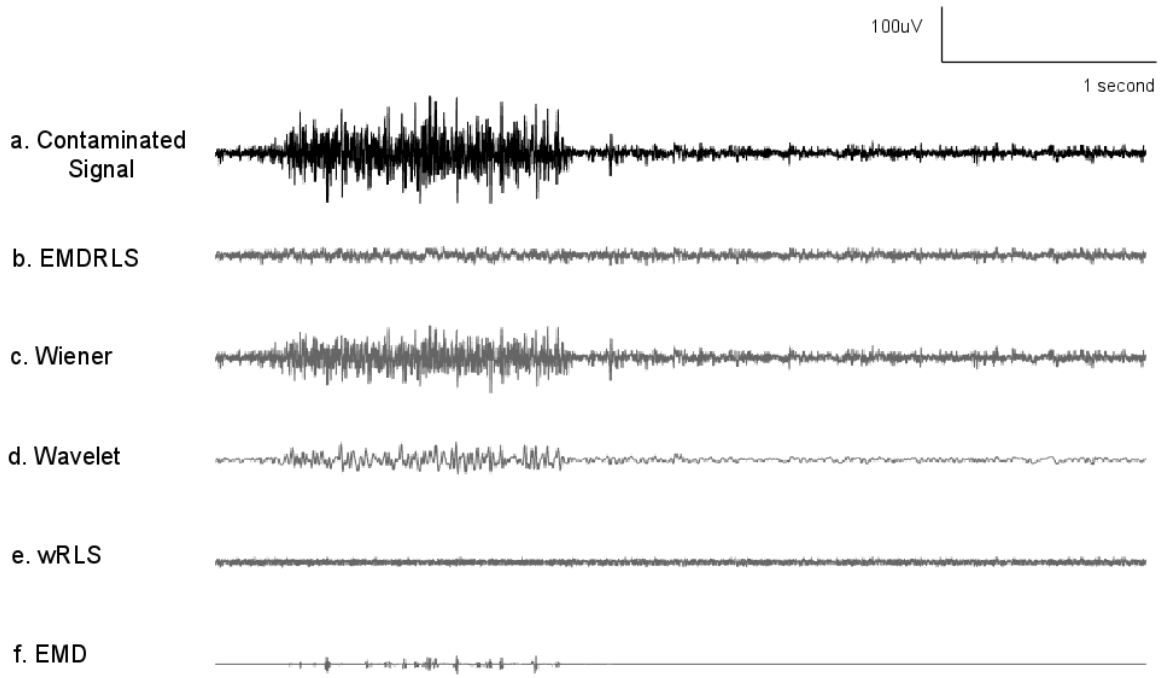

Figure 1: Typical waveforms of contaminated and filtered EEG signals for each filtering method (a - f). In this example, EEG detected at F3-F7 was corrupted by an EMG signal originating from the masseter muscle.

SNR analysis

Figure 2 shows the overall mean SNR of filtered signals for the level of contamination defined as: 1. SNR $\geq$ -5 dB, 2. -10 dB $\leq$ SNR $<$ -5 dB, 3. -20 dB $\leq$ SNR $<$ -10 dB, 4. -30 dB $\leq$ SNR $<$ -20 dB, and 5. SNR $<$ -30 dB. The results are shown for the frontal (Figure 2A) and masseter (Figure 2B) EMG contamination.

Figures 2A (frontal muscle) and 2B (masseter muscle) show the estimated relationship between the contamination level and the SNR of the filtered signal. The curves for each type of filter were obtained by fitting a spline model based on available data at the discrete points (i.e., from 1 to 5).

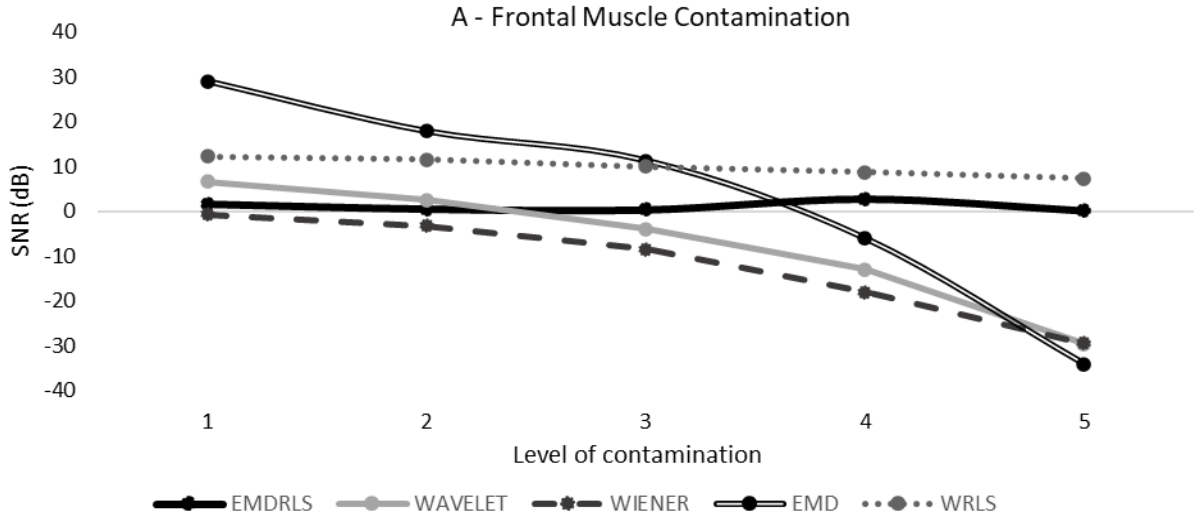

156

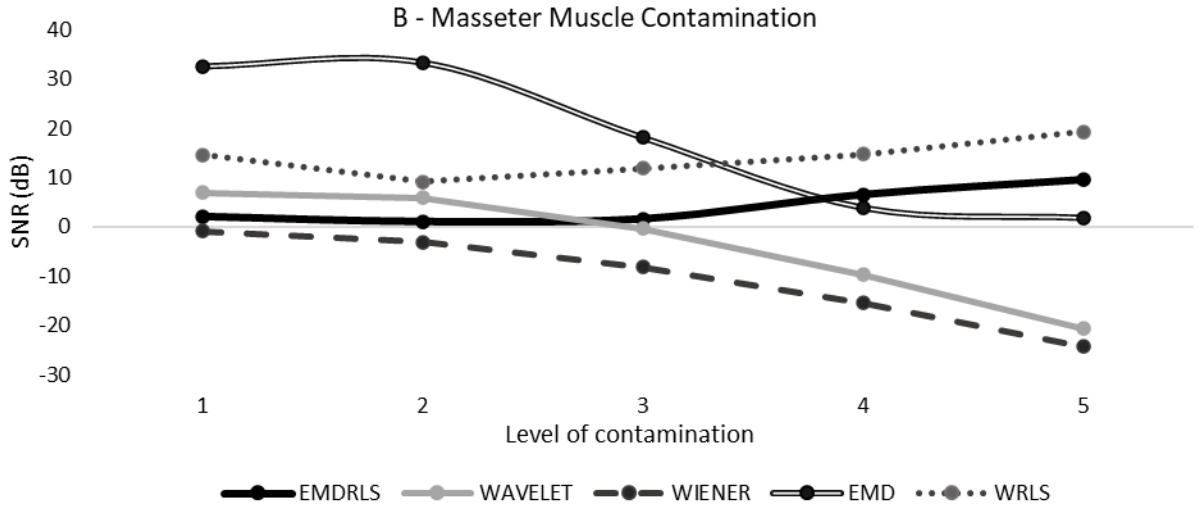

157

158 **Figure 2: Relationship between the contamination level and the SNR of the filtered signal contaminated**
159 **by the EMG from the frontal (A) and masseter (B) muscles.**

160 Figure 2A shows that the EMDRLS and wRLS techniques were less sensitive to a reduction in the contamination
161 level. The angle between the horizontal axis and the linear model fit for each curve of Figure 2A is -0.41°, -
162 9.42°, -44.41°, -50.60°, -64.24°, respectively for the methods EMDRLS, wRLS, EMD, wavelet and Wiener.

163 The estimated inclinations with respect to the horizontal axis for the curves of Figure 2B are 13.59°, 16.71°, -
164 39.08°, -44.46°, -50.45°, respectively for the methods wRLS, EMDRLS, Wiener, wavelet and EMD.

165 Figure 3A shows the overall mean SNR of the EMG contaminated signal after filtering by the EMG from the
166 frontal (A) and masseter (B) muscles with regard to the EEG sensor positioning. The overall mean SNR of the
167 corrupted EEG signal, s[n], is also shown.

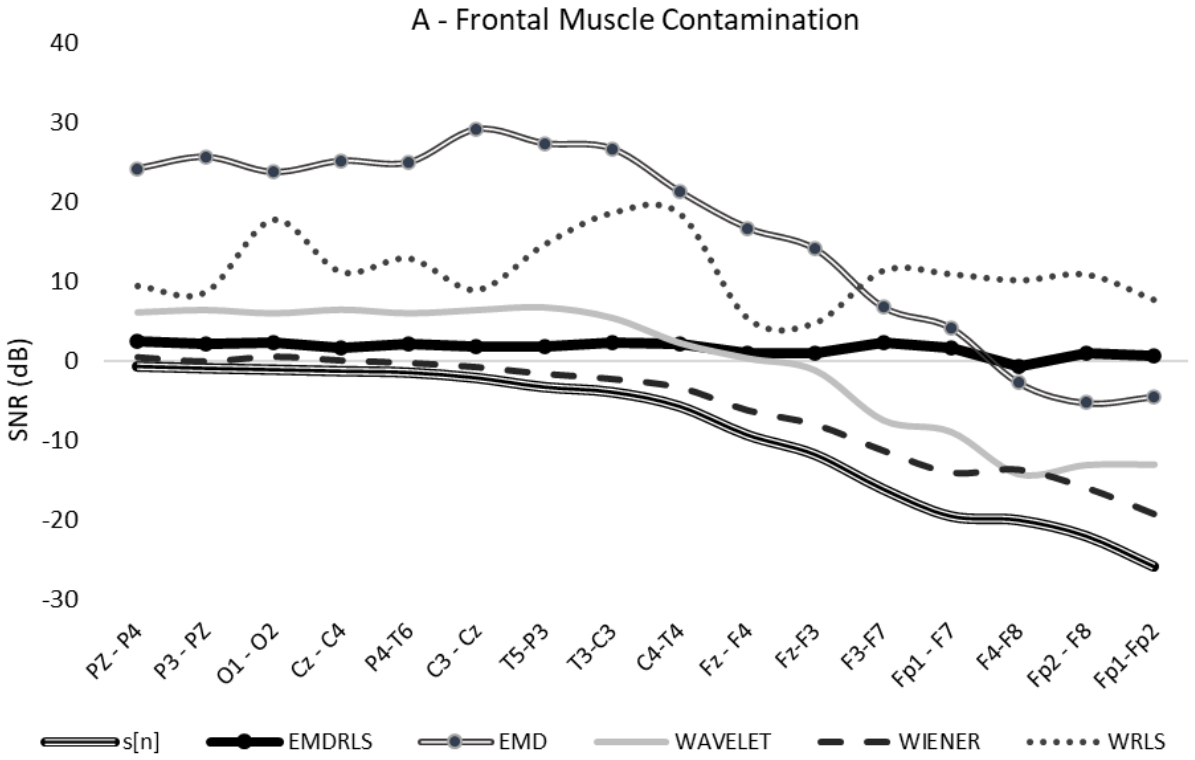

168

169

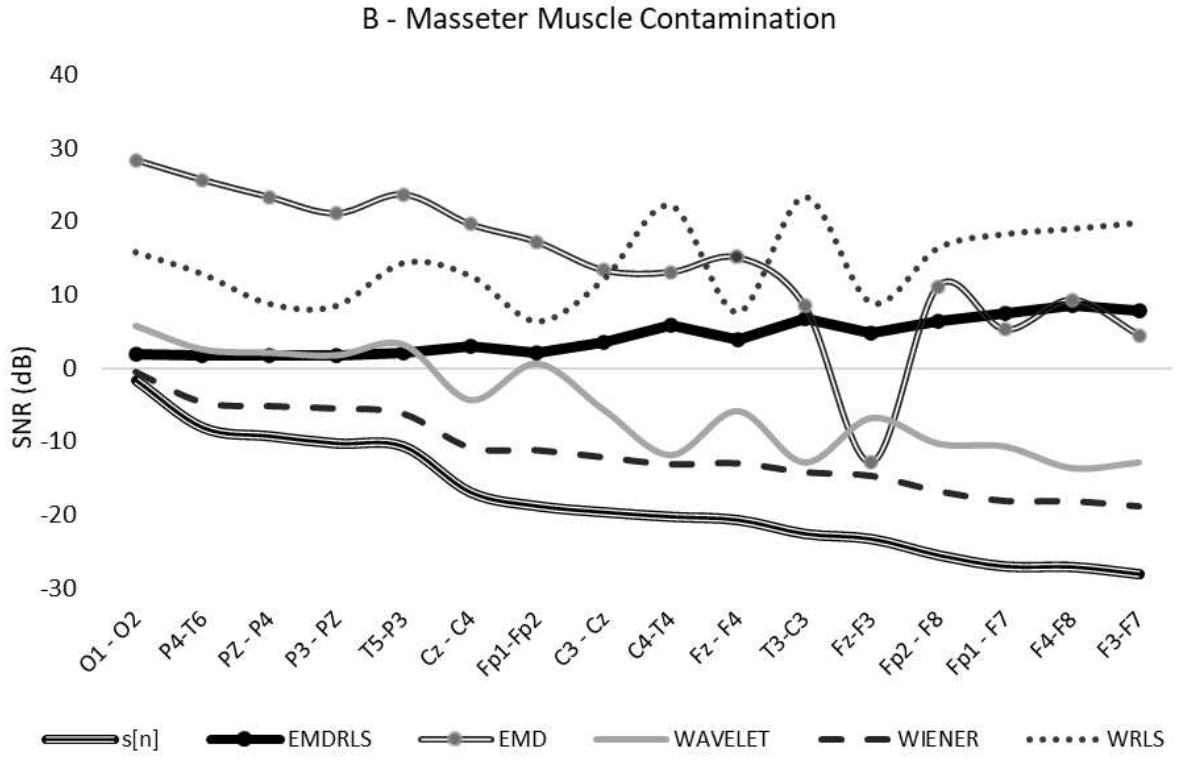

170

171 **Figure 3: Overall mean SNR of the filtered EMG from the frontal (A) and masseter (B) muscles in**
172 **relation to each EEG channel. The overall mean SNR of the contaminated EEG signal, s[n], is also shown.**

173

Ideally, the filter should be able to remove noise by maintaining signal information, regardless of the level of contamination. This can be achieved by a filter whose relationship between the level of contamination and the SNR of the filtered signal follows a linear model with a linear and angular coefficient close to zero in order to avoid degradation of the filtered signal at high levels of contamination. This scenario can be obtained when P_D equals P_C in Equation 6. To evaluate the performance of the filter by the dependence of the intensity of contamination, the Spearman's correlation coefficient between the SRN of the contaminated signal and the SNR of the filtered signal was calculated. Among the most contaminated channels (Fz-F3, F4-F8, F3-F7, Fp1-Fp2, T3-C3, C4-T4, Fp2-F8, and Fp1-F7) the correlation coefficient for the EMDRLS filtering method was 0.04 and -0.64, respectively for signals from the frontal and masseter. For the other methods, the correlation coefficient between the SNR of the filtered signal and the SNR of the frontal muscle contamination was 0.77, 0.82, 0.98, and 0.33, respectively for the methods EMD, wavelet, Wiener and wRLS. For the contamination from masseter, the correlation coefficient was 0.83, 0.93, 0.99 and -0.27, respectively for the methods EMD, wavelet, Wiener, and wRLS.

RMSE between the power spectrum of EMG-free EEG and filtered EEG epochs

Tables 1 and 2 show the overall mean RMSE values for the frontal and masseter muscles, respectively. Results for the frontal and central channels were included in the tables as they are the most contaminated.

The lower the RMSE the more efficient is the filter in terms of spectral preservation with regard to the EMG-free signal. The best results were obtained from the EMDRLS filter, which showed lower variability and significant differences for all frontal channels and EMG contamination from both muscles (i.e., frontal and masseter).

Table 1: Mean and standard deviation of the RMSE between the power spectrum of EMG-free EEG and filtered EEG epochs contaminated by EMG from the frontal muscle. The numeric labels in superscript denotes[(1-9)] significant difference between nonfiltered and filtered scenarios at a significance level of 0.05.

Channel	Frontal muscle (without filtering)	EMDRLS	EMD	Wiener	Wavelet	WRLS
Fp2 - F8	1.670 ±0.029[1,2]	0.039 ±*0.011*[1]	1.225 ±1.666	0.650 ±0.656	1.325 ±1.752	0.109 ±0.652[2]
F4-F8	1.311 ±0.060[3,4]	0.076 ±*0.093*[3]	0.995 ±1.546	0.446 ±0.436	1.166 ±1.611	0.091 ±0.109[4]
Fp1 - F7	1.251 ±0.019[5,6]	0.025 ±*0.024*[5]	0.737 ±1.491	0.636 ±1.001	0.658 ±0.976	0.074 ±0.039[6]
Fp1-Fp2	1.107 ±0.223[7,8]	0.013 ±*0.008*[7]	0.619 ±1.228	0.553 ±0.792	0.493 ±0.625	0.058 ±0.053[8]
C4-T4	0.708 ±1.355	0.140 ±*0.080*	0.618 ±0.629	0.387 ±0.670	0.643 ±1.126	0.422 ±0.314
F3-F7	0.580 ±0.066[9]	0.032 ±*0.021*[9]	0.219 ±0.314	0.284 ±0.249	0.388 ±0.275	0.081 ±0.049

Table 2: Mean and standard deviation of the RMSE between the power spectrum of EMG-free EEG and filtered EEG epochs contaminated by EMG from the masseter muscle. The numeric labels in superscript denotes significant difference between nonfiltered[(1-18)] and filtered scenarios at a significance level of 0.05

Channel	Masseter muscle (without filtering)	EMDRLS	EMD	Wiener	Wavelet	WRLS
C4-T4	8.047 ±3.596[1,2]	0.271 ±0.221[1]	0.338 ±0.353[2]	1.270 ±5.221	1.279 ±7.724	*0.290 ±0.430*
T3-C3	7.842 ±0.912[3,4]	*0.362 ±0.383[3]*	0.380 ±0.227	0.429 ±3.363	0.373 ±5.434	0.396 ±0.443[4]
F4-F8	5.388 ±0.189[5,6,7,8,9]	0.151 ±0.159[5]	0.159 ±0.155[6]	0.170 ±2.905[7]	0.181 ±3.555[8]	*0.155 ±0.181[9]*
F3-F7	4.571 ±1.107[10,11,12]	*0.158 ±0.119[10]*	0.260 ±0.053[11]	0.482 ±1.522	0.510 ±1.641	0.258 ±0.119[12]
Fp2 - F8	3.373 ±0.013 [13,14,15]	*0.109 ±0.105 [13]*	0.143 ±0.072[14]	0.175 ±1.519	0.179 ±1.600	0.151 ±0.099[15]
Fp1 - F7	3.345 ±0.150[16,17,18]	*0.134 ±0.125[16]*	0.186 ±0.055[17]	0.141 ±0.816	1.172 ±0.587	0.229 ±0.123[18]

Spectral preservation of brain rhythms

Tables 3 and 4 show the overall mean and standard deviation of MPSD for the frontal and masseter muscles, respectively. The table compares the MPSD for each brain rhythms between EMG-Free EEG signal and filtered signals. Only the proposed EMDRLS method did not produce differences between the noise free and the filtered signals for all brain rhythms.

Table 3: Mean and standard deviation of the MPSP (in µV) between the power spectrum of EMG-free EEG and filtered EEG epochs contaminated by frontal muscle EMG for the distinct brain rhythms. The effectiveness of filtering is measured by the spectral similarity between filtered EEG signals and the EMG-Free EEG signal. The numeric labels in superscript denotes[(1-11)] significant difference between the power spectrum of EMG-free EEG and filtered EEG epochs at a significance level of 0.05

Rythymn	EMG-free EEG	EMDRLS	WIENER	WAVELET	EMD	WRLS
Delta	0.041 ±0.035[1,2]	0.071 ±0.179	0.094 ±0.501[1]	0.113 ±0.3245	0.073 ±0.108	0.004 ±0.007[2]
Theta	0.071 ±0.0691[3,4]	0.087 ±0.106	0.135 ±0.724[3]	0.167 ±0.497	0.107 ±0.147	0.005 ±0.004[4]
Alpha	0.406 ±0.6321[5,6]	0.309 ±0.422	0.476 ±2.491[5]	0.908 ±2.678	0.483 ±0.748	0.015 ±0.021[6]
Beta	0.340 ±0.491[7,8]	0.304 ±0.419	0.374 ±1.532[7]	0.937 ±1.768	0.574 ±0.718	0.022 ±0.012[8]
Gamma	0.095 ±0.166[9,10,11]	0.092 ±0.147	0.257 ±0.721[9]	0.586 ±1.085[10]	0.356 ±0.594	0.014 ±0.006[11]

Table 4: Mean and standard deviation of the MPSP (in µV) between the power spectrum of EMG-free EEG and filtered EEG epochs contaminated by masseter muscle EMG for the distinct brain rhythms. The effectiveness of filtering is measured by the spectral similarity between filtered EEG signals and the

EMG-Free EEG signal. The numeric labels in superscript denotes[(1-13)] significant difference between the power spectrum of EMG-free EEG and filtered EEG epochs at a significance level of 0.05

Rythymn	EMG-free EEG	EMDRLS	WIENER	WAVELET	EMD	WRLS
Delta	0.056 ±0.058[1,2]	0.063 ±0.057	0.025 ±0.062[1]	0.136 ±0.269	0.089 ±0.125	0.002 ±0.001[2]
Theta	0.088 ±0.089[3,4]	0.096 ±0.084	0.035 ±0.085[3]	0.190 ±0.358	0.127 ±0.164	0.003 ±0.003[4]
Alpha	0.456 ±0.653[5,6]	0.360 ±0.467	0.117 ±0.302[5]	0.764 ±1.169	0.475 ±0.622	0.009 ±0.015[6]
Beta	0.388 ±0.579[7,8,9]	0.285 ±0.374	0.162 ±0.465[7]	1.943 ±3.979[8]	0.925 ±1.735	0.025 ±0.015[9]
Gamma	0.201 ±0.327[10,11,12,13]	0.122 ±0.203	0.124 ±0.290[10]	2.321 ±5.343[11]	1.090 ±2.400[12]	0.015 ±0.006[13]

Discussion

The EMDRLS method has been developed for the removal of facial muscular artifacts from EEG signals, which is an important requirement for distinct applications. It is a single channel approach for filtering low SNR EEG signals. In this research, EMD was used to generate an EMG noise reference to an adaptive RLS filter. The performance of the EMDRLS filter (Figure 5) was compared with other traditional single-channel approaches (wRLS, EMD, wavelet and Wiener) by using several quantitative metrics (SNR, RMSE and MPSD).

The developed filter was assessed on actual EEG data collected from 10 healthy subjects. Since there is a need for studies comparing the efficacy of filtering methods for different muscles [9,45], this research investigated the performance of the filter considering the EEG contamination by two distinct facial muscles (i.e., frontal and masseter).

Visual inspection of a typical EEG filtered signal (Figure 1) shows how the EMDRLS method guarantees the preservation of waveforms in the EMG-free region compared to other approaches and how EMG contamination is removed from the EEG signal.

From the results presented in Figures 2 and 3, the EMDRLS method is the less sensitive to the SNR of the corrupted EEG signal. Such results are consistent, independent of the noise produced by the frontal and masseter muscles, as measured by the relatively low slope of the linear model adjusted to the response curve of the EMDRLS method. This is further confirmed by the relatively low correlation coefficient (0.04 and -0.64, respectively, for the frontal and masseter) between the level of contamination and the SNR of the filtered signal. This low correlation reinforces relative independence of the method with regard to the contamination level.

Tables 1 and 2 compare the RMSE between EMG-free EEG and filtered EEG epochs contaminated by EMG from the frontal and masseter muscles. The selected EEG channels were those which presented the highest level of EMG contamination. The RMSE for the masseter is larger than the RMSE for the frontal muscle. This may be justified by the fact that the masseter is one of the strongest muscles (based on its weight) in the human body. The highest RMSE (i.e. 7.842 and 8.047) was obtained for the central regions of the scalp during the contraction of the masseter. These values were reduced to 0.362 (for T3-C3) and 0.271 (C4-T4) in the signals filtered by the EMDRLS method. The technique maintained the lowest RMSE values for all other channels (central and frontal) compared to other filtering techniques. Although there is no consensus among researchers on the selection of EEG artifact removal techniques, some researchers have proposed the use of the RMSE in the time domain [9,45,49]. In this research this metric was introduced to contrast the power spectrum between EMG-free EEG and EEG-filtered epochs.

When compared to the other filtering methods, the EMDRLS method was the one that produced the lowest mean RMSE with the lowest variability for all channels, suggesting spectral preservation. In addition, it was the only method that yielded statistical difference between the RMS of the nonfiltered and filtered signals for all EEG channels contaminated by EMG from the masseter muscle (Table 2). For EEG channels contaminated by EMG from the frontal muscle (Table 1) the results are similar, except for the RMSE of channel C4-T4 that was statistically equivalent to the RMSE of the nonfiltered signal. However, the RMSE value was significantly reduced from 0.708 to 0.140.

Tables 3 and 4 present the results for the metric MPSP. The desirable behavior of the filter is to guarantee a similarity of values between the MPSP of EMG-free EEG and filtered EEG epochs. The results in the tables are given for specific brain rhythms. The EMDRLS method was the only one that produced filtered EEG signals whose MPSP was statistically similar to the MPSP of the EMG-free EEG, for all brain rhythms.

The hybrid techniques analyzed in this study have combined the adaptive RLS filter with both EMD and wavelet decomposition techniques, which removed the EMG contamination as shown in Figure 1. However, the wRLS method does not preserve the waveform of the EMG-Free EEG signal. The superior performance of the hybrid technique with the EMD method is consistent with [54], which also compared both EMD and wavelet methods in a hybrid combination with ICA, and concluded that the wavelet-based hybrid technique performed worse than that based on EMD. The possible reason is that the wavelet analysis decomposes the signal at each stage in a predetermined way, excluding the possibility of adapting the decomposition to local variations of the oscillation. Without prior knowledge of the EMG-Free EEG signal, it is inconvenient to effectively select the ideal mother

wavelet and the number of decomposition levels. Conversely, hybrid filters with EMD are a completely data-oriented method, which means that the signal is decomposed in a natural way without requiring prior knowledge of the signal of interest. Therefore, EMD hybrid variations are generally preferred and have been widely used for EEG filtering as suggests in [18,30,31,43].

The technique known as Ensemble Empirical Mode Decomposition with Canonical Correlation Analysis (EEMD-CCA) combined with CCA in a single-channel approach as described by [43] was used to remove the EMG artifact for the EEG. This method has also been compared with the filtering methods based on wavelet, EMD and EEMD-ICA. The results have shown that the hybrid technique EEMD-CCA is a reliable and computationally efficient filter. However, they showed a relative improvement in the SNR below 4 dB, which contrasts with our work, which showed improvements in the SNR in the order of 20 dB in the frontal EEG channels. The same happens with the hybrid single-channel filter described by [30] which evaluated the EEMD-ICA technique, however, for low SNR (i.e., below 2 dB). Thus, although significant efforts have been made to develop methods for detecting and removing artifacts from EEG signals, this is still an active area of research.

Additional considerations regarding the ICA and CCA used in hybrid EMD filters must be taken into account as they could not be effective if the number of channels was not equal to the number of sources as described in [9]. According to [55], there is disagreement in the literature on the efficacy of ICA, especially for high frequencies, for the removal of EMG activity from the data, which is also reported in [56,57]. This was one of the factors that motivated the use of the adaptive RLS filter in this work for the removal of the EMG artifact.

The evaluation of the performance metrics together with the visual inspection of the filtered signals confirmed the robustness of the EMDRLS method. Future studies should consider the adaptation of the EMDRLS filter to real time applications and to the attenuation of other types of noise, for instance, motion. It is also necessary to extend the database of collected signals so that the filter can be evaluated under several other experimental conditions.

Conclusion

This paper has proposed an EMG signal denoising, the so-called EMDRLS. This type of filter fills the need for low SNR EEG filtering corrupted by facial EMG signals. The method was compared to other four single-channel filtering methods, i.e. Wiener, wavelet, EMD and a hybrid wavelet-RLS (wRLS) filter. The evaluation of the performance metrics showed the advantage of the use of the EMDRLS for single-channel EEG filtering corrupted by facial EMG. The current need is to adapt the use of the EMDRLS filter for real time application.

This would be relevant for the development of brain-computer interfaces and for studying the extraction information from EEG during facial muscular contraction.

Methods

Database and Participants

Data were collected from ten healthy individuals during the execution of successive facial muscular contractions to characterize the EEG signal contamination by facial muscular activity. This experimental protocol was based on previous published work [51] reporting the implementation of a facial EMG interface and motor learning assessment.

The EEG data in this study were obtained from the scalp surface of participants by using 16 channels in which the electrodes were positioned according to the standard 10-20 international placement. The signals were sampled at 5 kHz. The protocol consisted of two trials (i.e., trials 1 and 2 as illustrated in Figure 4). For each trial, the volunteer was asked to activate one of the following muscular groups: frontal (1) and masseter (2) muscles. These trials consisted of a sequence of 30 muscular contractions whose onset and duration were controlled by an auditory stimulus (beep). The beeps lasted 0.5 s, 1 s or 3 s, and the volunteer was asked to maintain the contraction while listening to the beep, and to finish the contraction immediately after the auditory stimulus. The stimuli were randomly and equally distributed. Figure 4 illustrates an example of stimuli during the experimental trials (1 and 2).

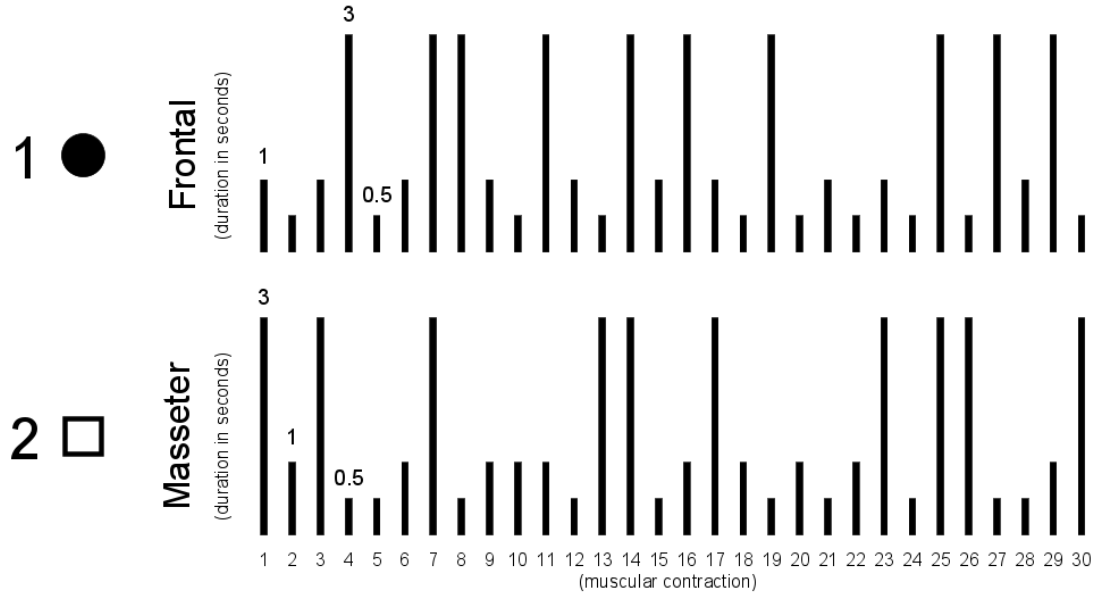

Figure 4: Example of an experiment with random sequences of auditory stimuli for the frontal (1 – circle) and masseter (2 - square) muscles. The vertical bars indicate the duration of the control auditory stimulus. The trial with the masseter muscle (2) starts after the end of the trial with the frontal muscle (1).

The EMDRLS Filtering Method

This section describes the EMDRLS technique proposed in this research. The use of this strategy for signal filtering has two main purposes: (1) to use EMD to generate noise activity, specific for each EEG channel, which is used as a reference signal to the RLS filter; and (2) to use RLS to filter noise corrupted EEG signals. The EMDRLS filter uses a single channel technique that is considered to be the most suitable for EEG filtering, as suggested by Chen [50].

The application of the EMDRLS consists of 3 steps as shown in Figure 5.

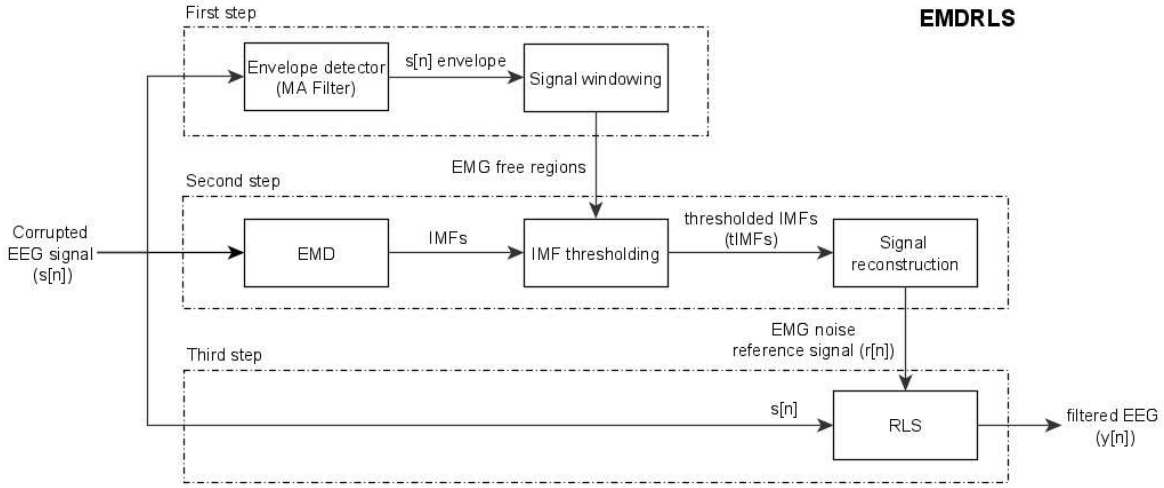

Figure 5: Block diagram of the EMDRLS technique for noise attenuation in EEG signals. First step: Signal regions without EMG are detected. Second step: The input signal s[n] is decomposed into IMFs and then the EMG-free regions are thresholded so that an EMG noise reference signal (r[n]) is generated. Third step: The input signal, s[n], is filtered by an RLS filter with a reference signal (r[n]), resulting in a filtered EEG signal (y[n]).

First step: detection of EMG-free signal regions

This step, illustrated in Figure 5, performs the detection of the facial muscular contraction. This information is used to identify EMG-free signal regions. EMG signal detection is based on the application of a moving average (MA) filter in which the window size L is equal to half of the sampling frequency (i.e., 5 kHz in this study).

The transfer function in the Z domain, H(z), of the employed MA filter is given in Eq. 1, where s is the raw EEG signal (Figure 5). The mean of the output of the MA filter was used as a threshold to detect EMG-free regions.

$$\mathrm{H}(z) = \frac{1}{L}\sum_{k=0}^{L-1} s[k]z^{-k} \quad (1)$$

Second step: generation of the EMG noise reference signal

EMD was used to decompose the contaminated signal s[n] into M limited band components $d_m[n]$ known as Intrinsic Mode Functions (IMFs) [58] defined in accordance with the following conditions:

(i) In the whole time-series, the number of extrema and number of zero crossings must be either equal or differ at most by 1.

(ii) At any point in the time-series, the mean value of the envelopes, one defined by the local maxima (upper envelope) and other by the local minima (lower envelope), is 0. This mean is computed for all available samples in the time-series.

The signal $\boldsymbol{s}[\boldsymbol{n}]$ can be represented by Eq. 2.

$$\mathrm{s[n]} = \sum_{m=1}^{M} d_m[n] + r_M[n] \quad (2)$$

where $d_m[n]$ is the *m-th* IMF, and $r_M[n]$ is the final residue which can be a constant or an average trend.

As EMD provides the decomposition of a signal into different time scales or IMFs, it is possible to filter the signal components individually instead of the original signal. Thus, the following procedure is applied to filter EEG signals:

1. Decompose the signal into IMFs
2. Threshold the estimated IMFs using the EMG-free epochs as noise
3. Reconstruct the signal r[n] to obtain an EMG noise reference signal as a linear summation of the thresholded IMFs

The strategy used for IMF thresholding is the soft-thresholding technique applied to individual IMFs, as shown in Eq. 3 [59], in which $tIMF_m$ is the denoised (or thresholded) version of the m-th IMF. The threshold t_m is estimated by using the following strategy: a window of noise is selected from the original signal and then the boundaries of this window are used to extract a region of noise from IMFs. The standard deviation of each region is then estimated and taken as the required thresholds t_m (t_1, ..., t_M).

$$tIMF_m sign(IMF_m) = (|IMF_m| - t_m)_+ \quad (3)$$

Third step: RLS adaptative filtering

The adaptive RLS filtering [35,52,53] is depicted in Figure 5. The input signal s[n] is composed of two components, i.e., EEG and EMG artifact. The reference signal, r[n], necessary for RLS filtering is estimated as described previously. The application of the RLS filter assumes that the desired EEG and the noise are independent (or at least uncorrelated) [60]. The output of this system, y[n], is the filtered EEG signal.

Comparative analysis with single-channel methods

The EMDRLS method is compared to the following single-channel artifact removal methods: (i) Wavelet, (ii) Wiener (iii) EMD and (iv) Hybrid wavelet-RLS (wRLS).

The wavelet filter was used as suggested in [61]. In this study, Daubechies 8 (db8) was identified as the most suitable to eliminate noise from EEG signals. In addition, it was applied 5 levels of decomposition and a soft threshold. The Wiener filter used was based on the two-step noise reduction technique for EEG filtering proposed in [62]. The EMD filter was used to filter EEG as suggested in [13] by means of thresholded IMFs. The wRLS hybrid method was used in accordance to [63,64] that illustrates its application to remove ocular artifacts from EEG.

Performance metrics

The aim of the use of performance metrics is the objective evaluation of noise removal capability of each investigated method.

To evaluate the performance of the aforementioned EEG filtering methods, the following metrics were used: (i) the signal-noise ratio (SNR) of the contaminated signal, (ii) the root mean square error (RMSE) between the power spectrum of artifact free and filtered EEG epochs, (iii) the spectral preservation of brain rhythms (i.e., delta, theta, alpha, beta, and gamma rhythms) of filtered signals.

Figure 6 defines the signal regions A, B, C and D for the estimation of performance metrics: s[n] is the corrupted signal and y[n] the corresponding filtered version. A is the signal region corrupted by EMG, whereas C is the corresponding filtered signal. B is the EMG-free region, and D the corresponding filtered signal.

Eq. 4 defines the mean power (P_{epoch}) of each region, in which V is the input discrete time series and N is the number of samples of the signal. SNR_{in} (Eq. 5) measures the SNR with respect to the regions A and B of the contaminated signal s[n], whereas SNR_{out} (Eq. 6) measures the SNR with respect to the regions C and D of the filtered signal.

$$P_{epoch} = \sum_{n=1}^{N} \frac{V[n]^2}{N} \tag{4}$$

$$SNR_{in} = 10log_{10}\left(\frac{P_B}{P_A}\right) \tag{5}$$

$$SNR_{out} = 10log_{10}\left(\frac{P_D}{P_C}\right) \tag{6}$$

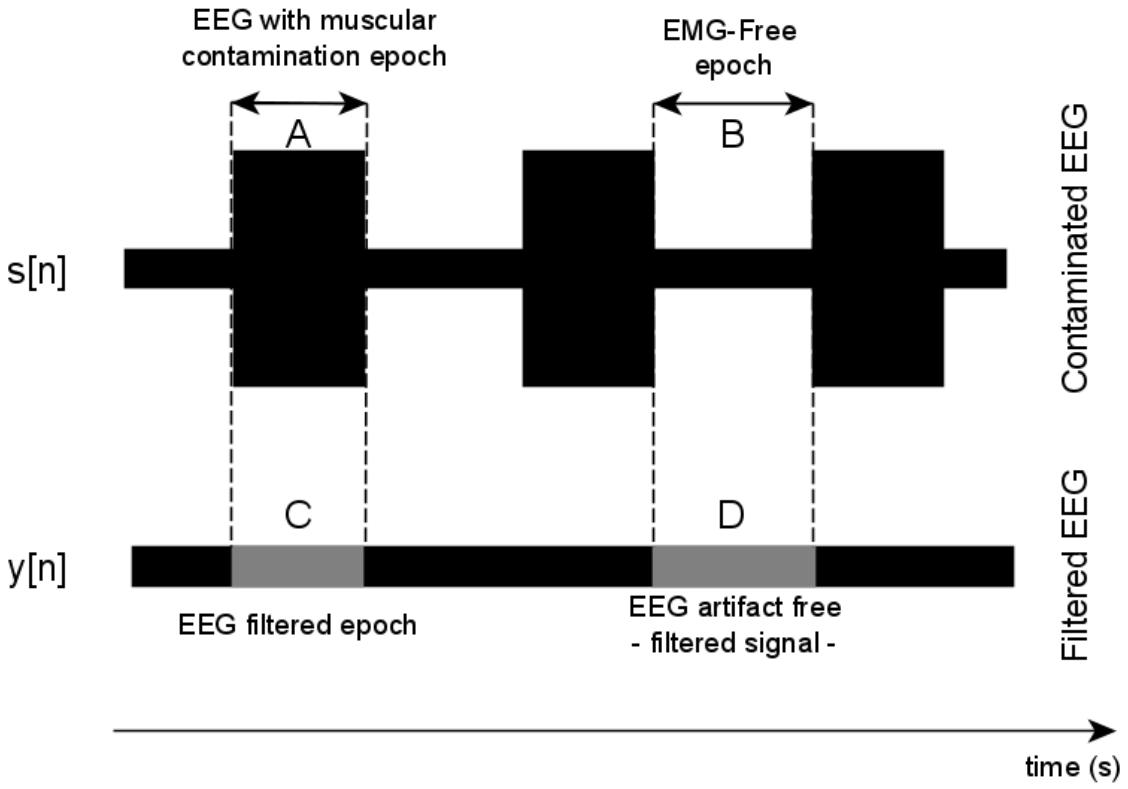

394

395 **Figure 6: Definition of signal regions (A, B, C and D) for the estimation of the performance metrics. s[n] is**
396 **the corrupted signal and y[n] is its corresponding filtered version. A is the signal region corrupted by**
397 **EMG, whereas C is the corresponding filtered signal. B is the EMG-free region and D the corresponding**
398 **filtered signal.**

399

400 RMSE provides a distance measurement between the power spectrum of EMG-free and filtered EEG epochs**.**
401 The power spectral density of each signal is obtained by the Burg's method [65]. The Burg's method, also
402 known as the Maximum Entropy Method (MEM) consists of minimizing the sum squared of both the forward
403 and the backward prediction errors. The spectrum is resulted by derivative of the Lagrange function where
404 Fourier transform coefficients are replaced by Lagrange multipliers, after maximizing the entropy function [66].

405 Eq. 7 defines the $RMSE_{in}$, which is the distance measurement between the power spectral density of EMG-free
406 EEG, X(f), and contaminated EEG epochs, R(f). Eq. 8 defines the $RMSE_{out}$ as a distance measurement between
407 the power spectral density of the EMG-free EEG epoch, X(f), and filtered EEG epochs, Y(f).

408

$$RMSE_{in} = \sqrt{\frac{1}{N}\sum_{f=1}^{F}\big(X(f) - R(f)\big)^2} \quad (7)$$

where N = F, which is the length of vectors $X(f)$ and $R(f)$.

$$RMSE_{out} = \sqrt{\frac{1}{N}\sum_{f=1}^{F}\big(X(f) - Y(f)\big)^2} \quad (8)$$

where N = F, which is the length of vectors $X(f)$ and $Y(f)$.

One-sample Kolmogorov-Smirnov test was employed to test the normality of RMSE ($p < 0.05$), rejecting the hypothesis that the data distribution is normal. Thus, the non-parametric Kruskal-Wallis test was used to verify the statistical difference ($p < 0.05$) between $RMSE_{in}$ and $RMSE_{out}$ for the five filtering methods. Also, the Tukey-Kramer post-hoc test was used for a pairwise comparison between methods.

The mean Burg's power spectral density (MPSD) was estimated for the evaluation of the spectral preservation of brain rhythms (i.e., delta, theta, alpha, beta, and gamma) of filtered signals. An overall average of the MPSD was calculated for the contaminated signal s[n], the filtered signal y[n] and the EMG-free epochs.

One-sample Kolmogorov-Smirnov test was employed to test the normality of MPSP ($p < 0.05$), rejecting the hypothesis that the data distribution is normal. Thus, the non-parametric Kruskal-Wallis test was used to verify the statistical difference ($p < 0.05$) between MPSD estimated from regions B and C and regions B and D illustrated in Figure 6, and the Tukey-Kramer post-hoc test was used was used for a pairwise comparison between methods.

List of abbreviations

EMG - electromyography

EEG - electroencephalogram

BCI - brain-computer interface

SNR - signal to noise ratio

RMSE - root-mean-square error

ICA - independent component analysis

CCA - canonical correspondence analysis

BSS - blind signal separation

WT - wavelet transform

EMD - empirical mode decomposition

DWT - discrete wavelet transform

EOG - electrooculogram

wRLS - wavelet with recursive least squares

MEM - maximum entropy method

MA - moving average

UFU - Federal University of Uberlândia

Declarations

Ethics approval and consent to participate

This study follows the Resolution 466/2012 of the National Health Council. The study was conducted at the Centre for Innovation and Technology Assessment in Health of the Federal University of Uberlândia (UFU), Brazil. The protocols were approved by the Human Research Ethics Committee (CEP-UFU), CAAE Number: 43670815.4.0000.5152

Consent for publication

The authors have the consent for publication form by all people with the authorization to publish the collected data.

Availability of data and materials

The datasets used during the current study are available from the corresponding author on reasonable request.

Competing interests

The authors declare that they have no competing interests

Funding

Not applicable

Authors' contributions

GMD is the leading researcher, responsible for data collection, code implementation, data analysis, paper writing. This study is the result of his PhD thesis. CMMQ, LBP, LMDL and SCC are the responsible for hardware set up, recruitment of participants and data collection. Participated in the revision of the paper. SW, AAP and MFV participated in the writing and revision of the paper. Contributed to the data analysis and supervision of students. KCF participated in the revision of the paper. AOA is the main supervisor of the research. Responsible for the design of the study, supervision of students, data analysis, writing and revision of the paper.

Acknowledgement

The present work was carried out with the support of the National Council for Scientific and Technological Development (CNPq – Project 304818/2018-6), Coordination for the Improvement of Higher Education Personnel (CAPES Program CAPES/DFATD-88887.159028/2017-00, Program CAPES/COFECUB-88881.370894/2019-01) and the Foundation for Research Support of the State of Minas Gerais (FAPEMIG-APQ-00942-17). A. O. Andrade, A. A. Pereira and M. F. Vieira are a fellow of CNPq, Brazil (304818/2018-6, 310911/2017-6, and 306205/2017-3).

Conflict of interest

The authors declare that they have no conflict of interest.

Footnotes

Not applicable

References

1. Niedermeyer E, da Silva FHL. Electroencephalography: basic principles, clinical applications, and related fields. Baltimore: Williams & Williams; 2005.

2. Foxe JJ, Snyder AC. The role of alpha-band brain oscillations as a sensory suppression mechanism during selective attention. Front Psychol. 2011;2. doi:10.3389/fpsyg.2011.00154

3. Ramadan RA, Vasilakos A V. Brain computer interface: control signals review. Neurocomputing. 2017;223: 26–44. doi:10.1016/j.neucom.2016.10.024

4. Mihajlovic V, Grundlehner B, Vullers R, Penders J. Wearable, wireless EEG solutions in daily life applications: What are we missing? IEEE J Biomed Heal Informatics. 2015;19: 6–21. doi:10.1109/JBHI.2014.2328317

5. Abo-Zahhad M, Ahmed SM, Abbas SN. A New EEG Acquisition Protocol for Biometric Identification Using Eye Blinking Signals. Int J Intell Syst Appl. 2015;7: 48–54. doi:10.5815/ijisa.2015.06.05

6. Hero A. Signal processing identity [President's message]. IEEE Signal Process Mag. 2006;23: 4–4. doi:10.1109/MSP.2006.1657808

7. Silva GEG, Valença MOS. Neurologia Clínica. Recife: Editora Universitária da Universidade Federal De Pernambuco (UFPE); 2003.

8. Sweeney KT, Ward TE, McLoone SF. Artifact Removal in Physiological Signals—Practices and Possibilities. IEEE Trans Inf Technol Biomed. 2012;16: 488–500. doi:10.1109/TITB.2012.2188536

9. Urigüen JA, Garcia-Zapirain B. EEG artifact removal—state-of-the-art and guidelines. J Neural Eng. 2015;12: 031001. doi:10.1088/1741-2560/12/3/031001

10. Tatum WO, Dworetzky BA, Schomer DL. Artifact and recording concepts in EEG. J Clin Neurophysiol. 2011;28: 252–263. doi:10.1097/WNP.0b013e31821c3c93

11. Nunez PL, Srinivasan R. Electric Fields of the Brain. Nova York: Oxford University Press; 2006. doi:10.1093/acprof:oso/9780195050387.001.0001

12. Goncharova II, McFarland DJ, Vaughan TM, Wolpaw JR. EMG contamination of EEG: Spectral and topographical characteristics. Clin Neurophysiol. 2003;114: 1580–1593. doi:10.1016/S1388-2457(03)00093-2

13. Safieddine D, Kachenoura A, Albera L, Birot G, Karfoul A, Pasnicu A, et al. Removal of muscle artifact from EEG data: comparison between stochastic (ICA and CCA) and deterministic (EMD and wavelet-based) approaches. EURASIP J Adv Signal Process. 2012;2012: 127. doi:10.1186/1687-6180-2012-127

14. Bono V, Das S, Jamal W, Maharatna K. Hybrid wavelet and EMD/ICA approach for artifact suppression in pervasive EEG. J Neurosci Methods. 2016;267: 89–107. doi:10.1016/j.jneumeth.2016.04.006

15. Frølich L, Dowding I. Removal of muscular artifacts in EEG signals: a comparison of linear decomposition methods. Brain Informatics. 2018. doi:10.1007/s40708-017-0074-6

16. Gabsteiger F, Leutheuser H, Reis P, Lochmann M, Eskofier BM. ICA-based reduction of electromyogenic artifacts in EEG data: Comparison with and without EMG data. 2014 36th Annual International Conference of the IEEE Engineering in Medicine and Biology Society. IEEE; 2014. pp. 3861–3864. doi:10.1109/EMBC.2014.6944466

17. Upadhyay R, Padhy PK, Kankar PK. EEG artifact removal and noise suppression by Discrete Orthonormal S-Transform denoising. Comput Electr Eng. 2016;53: 125–142. doi:10.1016/j.compeleceng.2016.05.015

18. Mucarquer JA, Prado P, Escobar M-J, El-Deredy W, Zanartu M. Improving EEG Muscle Artifact Removal With an EMG Array. IEEE Trans Instrum Meas. 2020;69: 815–824. doi:10.1109/TIM.2019.2906967

19. Correa AG, Laciar E., Patiño HD., Valentinuzzi ME. Artifact removal from EEG signals using adaptive filters in cascade. J Phys Conf Ser. 2007; 10. doi:10.1088/1742-6596/90/1/012081

20. Kher R, Gandhi R. Adaptive filtering based artifact removal from electroencephalogram (EEG) signals. 2016 International Conference on Communication and Signal Processing (ICCSP). IEEE; 2016. pp. 0561–0564. doi:10.1109/ICCSP.2016.7754202

21. Ferdous MJ, Ali S. A Comparison of Wiener and Kalman Filters for the Artifact Suppression from EEG Signal. Int J Sci Res. 2017;6: 2029–2035. doi:10.21275/ART20172896

22. Maki H, Toda T, Sakti S, Neubig G, Nakamura S. EEG signal enhancement using multi-channel wiener filter with a spatial correlation prior. 2015 IEEE Int Conf Acoust Speech Signal Process. 2015; 2639–2643. doi:10.1109/ICASSP.2015.7178449

23. Morbidi F, Garulli A, Prattichizzo D, Rizzo C, Rossi S. Application of Kalman filter to remove TMS-induced artifacts from EEG recordings. IEEE Trans Control Syst Technol. 2008;16: 1360–1366. doi:10.1109/TCST.2008.921814

24. Albera L, Kachenoura A, Comon P, Karfoul A, Wendling F, Senhadji L, et al. ICA-based EEG denoising: A comparative analysis of fifteen methods. Bull Polish Acad Sci Tech Sci. 2012;60: 407–418. doi:10.2478/v10175-012-0052-3

25. James C, Hesse C. Independent component analysis for biomedical signals. Physiol Meas. 2005;26: R15. doi:doi: 10.1088/0967-3334/26/1/r02

539 26. Turnip A, Pardede J. Artefacts Removal of EEG Signals with Wavelet Denoising. 2017;00058: 1–10.
540 doi:10.1051/matecconf/201713500058

541 27. Ngoc PP, Hai VD, Bach NC, Binh P Van. EEG Signal Analysis and Artifact Removal by Wavelet
542 Transform. 2015; 179–183. Available: http://link.springer.com/chapter/10.1007/978-3-319-11776-8_44

543 28. Alam ME, Samanta B. Performance Evaluation of Empirical Mode Decomposition for EEG Artifact
544 Removal. Volume 4B: Dynamics, Vibration, and Control. ASME; 2017. p. V04BT05A024.
545 doi:10.1115/IMECE2017-71647

546 29. Gaur P, Pachori RB, Hui Wang, Prasad G. An empirical mode decomposition based filtering method for
547 classification of motor-imagery EEG signals for enhancing brain-computer interface. 2015 International
548 Joint Conference on Neural Networks (IJCNN). IEEE; 2015. pp. 1–7. doi:10.1109/IJCNN.2015.7280754

549 30. Zeng K, Chen D, Ouyang G, Wang L, Liu X, Li X. An EEMD-ICA Approach to Enhancing Artifact
550 Rejection for Noisy Multivariate Neural Data. IEEE Trans Neural Syst Rehabil Eng. 2016;24: 630–638.
551 doi:10.1109/TNSRE.2015.2496334

552 31. Chen X, He C, Peng H. Removal of muscle artifacts from single-channel EEG based on ensemble
553 empirical mode decomposition and multiset canonical correlation analysis. J Appl Math. 2014;2014.
554 doi:10.1155/2014/261347

555 32. Salsabili S, Sardoui SH, Shamsollahi MB. Interictal EEG Denoising using Independent Component
556 Analysis and Empirical Mode Decomposition. 2015; 0–5.

557 33. Daly I, Scherer R, Billinger M, Muller-Putz G. FORCe: Fully Online and Automated Artifact Removal
558 for Brain-Computer Interfacing. IEEE Trans Neural Syst Rehabil Eng. 2015;23: 725–736.
559 doi:10.1109/TNSRE.2014.2346621

560 34. Kim M, Kim S-P. A comparsion of artifact rejection methods for a BCI using event related potentials.
561 2018 6th International Conference on Brain-Computer Interface (BCI). IEEE; 2018. pp. 1–4.
562 doi:10.1109/IWW-BCI.2018.8311530

563 35. Gerardo J, C. J, Velazquez J. Applications of Adaptive Filtering. Adaptive Filtering Applications.
564 InTech; 2011. pp. 1–20. doi:10.5772/16873

565 36. Chaves MLF, Finkelsztejn A, Stefani MA. Eletroencefalografia. Rotinas em neurologia e neurocirurgia.
566 Artmed Editora; 2008.

37. Sengupta SK, Kay SM. Fundamentals of Statistical Signal Processing: Estimation Theory. Technometrics. 1995;37: 465. doi:10.2307/1269750

38. Gao J, Sultan H, Jing Hu, Wen-Wen Tung. Denoising Nonlinear Time Series by Adaptive Filtering and Wavelet Shrinkage: A Comparison. IEEE Signal Process Lett. 2010;17: 237–240. doi:10.1109/LSP.2009.2037773

39. Iyer D, Zouridakis G. Single-trial evoked potential estimation: Comparison between independent component analysis and wavelet denoising. Clin Neurophysiol. 2007;118: 495–504. doi:10.1016/j.clinph.2006.10.024

40. Krishnaveni V, Jayaraman S, Anitha L, Ramadoss K. Removal of ocular artifacts from EEG using adaptive thresholding of wavelet coefficients. J Neural Eng. 2006;3: 338–346. doi:10.1088/1741-2560/3/4/011

41. Rutledge DN, Jouan-Rimbaud Bouveresse D. Independent Components Analysis with the JADE algorithm. TrAC Trends Anal Chem. 2013;50: 22–32. doi:10.1016/j.trac.2013.03.013

42. Zhang C, Yang J, Lei Y, Ye F. Single channel blind source separation by combining slope ensemble empirical mode decomposition and independent component analysis. J Comput Inf Syst. 2012;8: 3117–3126.

43. Sweeney KT, McLoone SF, Ward TE. The Use of Ensemble Empirical Mode Decomposition With Canonical Correlation Analysis as a Novel Artifact Removal Technique. IEEE Trans Biomed Eng. 2013;60: 97–105. doi:10.1109/TBME.2012.2225427

44. Sweeney-Reed CM, Nasuto SJ, Vieira MF, Andrade AO. Empirical Mode Decomposition and its Extensions Applied to EEG Analysis: A Review. Adv Data Sci Adapt Anal. 2018;10: 1840001. doi:10.1142/S2424922X18400016

45. Mannan MMN, Jeong MY, Kamran MA. Hybrid ICA—Regression: Automatic Identification and Removal of Ocular Artifacts from Electroencephalographic Signals. Front Hum Neurosci. 2016;10. doi:10.3389/fnhum.2016.00193

46. Sweeney K. Motion Artifact Processing Techniques for Physiological Signals. 2013.

47. Castellanos NP, Makarov VA. Recovering EEG brain signals: Artifact suppression with wavelet enhanced independent component analysis. J Neurosci Methods. 2006;158: 300–312.

595 doi:10.1016/j.jneumeth.2006.05.033

596 48. Somers B, Francart T, Bertrand A. A generic EEG artifact removal algorithm based on the multi-channel
597 Wiener filter. J Neural Eng. 2018;15: 036007. doi:10.1088/1741-2552/aaac92

598 49. Saini M, Satija U, Upadhayay MD. Effective automated method for detection and suppression of muscle
599 artefacts from single-channel EEG signal. Healthc Technol Lett. 2020;7: 35–40.
600 doi:10.1049/htl.2019.0053

601 50. Chen X, Liu A, Chiang J, Wang ZJ, McKeown MJ, Ward RK. Removing Muscle Artifacts from EEG
602 Data: Multichannel or Single-Channel Techniques? IEEE Sens J. 2016;16: 1986–1997.
603 doi:10.1109/JSEN.2015.2506982

604 51. Andrade AOAO, Pereira AAA, Jr CGPCGP, Kyberd PJPJ. Mouse emulation based on facial
605 electromyogram. Biomed Signal Process Control. 2013;8: 142–152. doi:10.1016/j.bspc.2012.09.001

606 52. Bellanger MG. Fast Least Squares Transversal Adaptive Filters. Adaptive Digital Filters. New York:
607 Marcel Dekker; 2001.

608 53. Diniz PSR. Adaptive Filtering. Boston, MA: Springer US; 2008. doi:10.1007/978-0-387-68606-6

609 54. Mijović B, De Vos M, Gligorijević I, Taelman J, Van Huffel S. Source Separation From Single-Channel
610 Recordings by Combining Empirical-Mode Decomposition and Independent Component Analysis. IEEE
611 Trans Biomed Eng. 2010;57: 2188–2196. doi:10.1109/TBME.2010.2051440

612 55. Muthukumaraswamy SD. High-frequency brain activity and muscle artifacts in MEG/EEG: a review and
613 recommendations. Front Hum Neurosci. 2013;7. doi:10.3389/fnhum.2013.00138

614 56. McMenamin BW, Shackman AJ, Greischar LL, Davidson RJ. Electromyogenic artifacts and
615 electroencephalographic inferences revisited. Neuroimage. 2011;54: 4–9.
616 doi:10.1016/j.neuroimage.2010.07.057

617 57. Olbrich S, Jödicke J, Sander C, Himmerich H, Hegerl U. ICA-based muscle artefact correction of EEG
618 data: What is muscle and what is brain? Neuroimage. 2011;54: 1–3.
619 doi:10.1016/j.neuroimage.2010.04.256

620 58. Huang NE, Shen Z, Long SR, Wu MC, Snin HH, Zheng Q, et al. The empirical mode decomposition and
621 the Hubert spectrum for nonlinear and non-stationary time series analysis. Proc R Soc A Math Phys Eng

622 Sci. 1998;454: 903–995. doi:10.1098/rspa.1998.0193

623 59. Andrade AO, Nasuto S, Kyberd P, Sweeney-Reed CM, Van Kanijn FR. EMG signal filtering based on
624 Empirical Mode Decomposition. Biomed Signal Process Control. 2006;1: 44–55.
625 doi:10.1016/j.bspc.2006.03.003

626 60. Pivik RT, Broughton RJ, Coppola R, Davidson RJ, Fox N, Nuwer MR. Guidelines for the recording and
627 quantitative analysis of electroencephalographic activity in research contexts. Psychophysiology.
628 1993;30: 547–558. doi:10.1111/j.1469-8986.1993.tb02081.x

629 61. Mamun M, Al-Kadi M, Marufuzzaman M. Effectiveness of Wavelet Denoising on
630 Electroencephalogram Signals. J Appl Res Technol. 2013;11: 156–160. doi:10.1016/S1665-
631 6423(13)71524-4

632 62. Plapous C, Marro C, Scalart P. Improved Signal-to-Noise Ratio Estimation for Speech Enhancement.
633 IEEE Trans Audio, Speech Lang Process. 2006;14: 2098–2108. doi:10.1109/TASL.2006.872621

634 63. Kumar PS, Arumuganathan R, Sivakumar K, Vimal C. Removal of artifacts from EEG signals using
635 adaptive filter through wavelet transform. 2008 9th International Conference on Signal Processing.
636 IEEE; 2008. pp. 2138–2141. doi:10.1109/ICOSP.2008.4697569

637 64. Babu PA, Prasad KVSVR. Removal of Ocular Artifacts from EEG Signals by Fast RLS Algorithm using
638 Wavelet Transform. Int J Comput Appl. 2011;21: 1–5. doi:10.5120/2503-3384

639 65. Orfanidis SJ. Optimum Signal Processing. 2nd ed. Piscataway, NJ, United States: McGraw-Hill
640 Publishing Company; 2007.

641 66. Singh VP. Entropy Spectral Analyses. Entropy Theory and its Application in Environmental and Water
642 Engineering. Chichester, UK: John Wiley & Sons, Ltd; 2013. pp. 436–491.
643 doi:10.1002/9781118428306.ch11

644

Figures

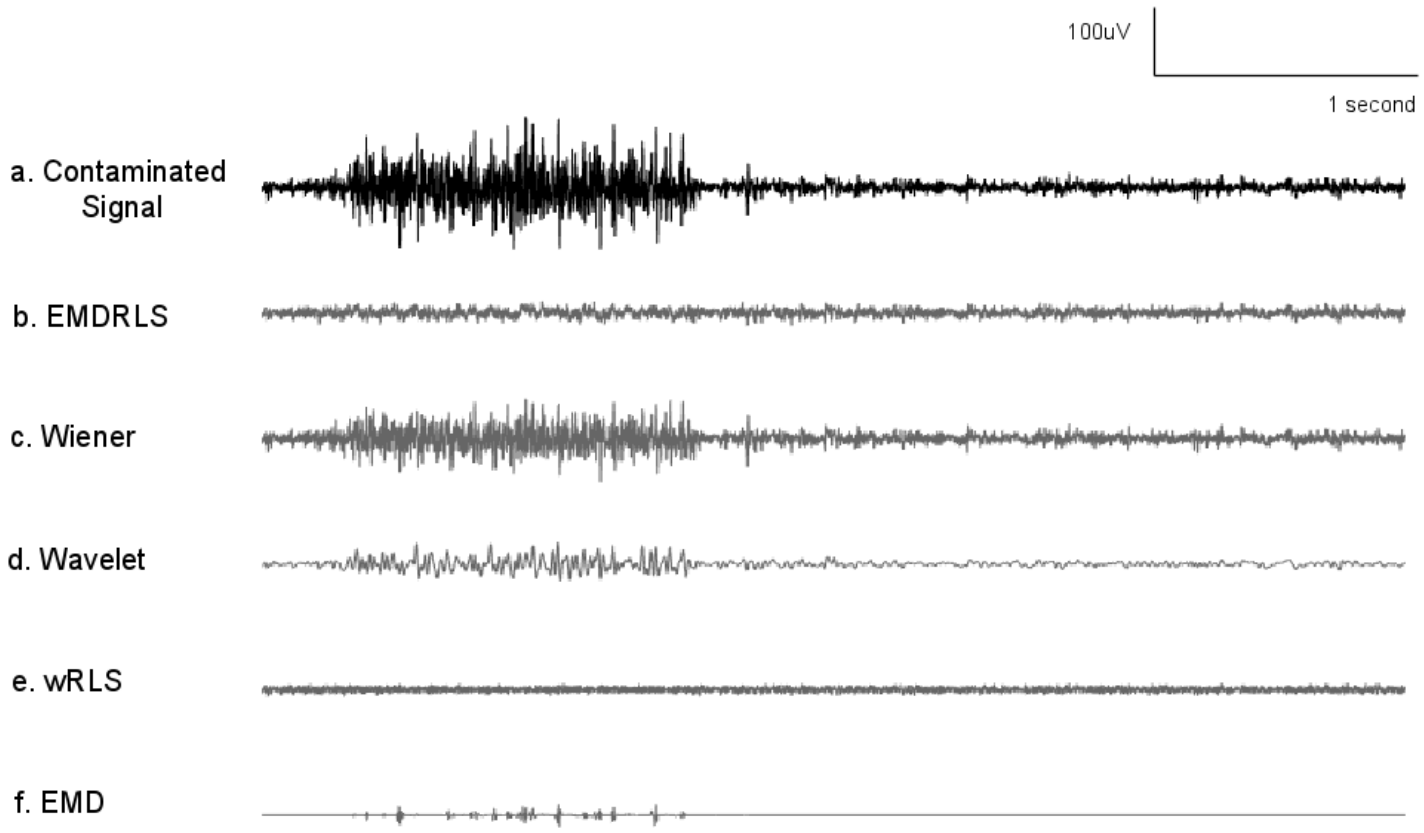

Figure 1

Typical waveforms of contaminated and filtered EEG signals for each filtering method (a - f). In this example, EEG detected at F3-F7 was corrupted by an EMG signal originating from the masseter muscle.

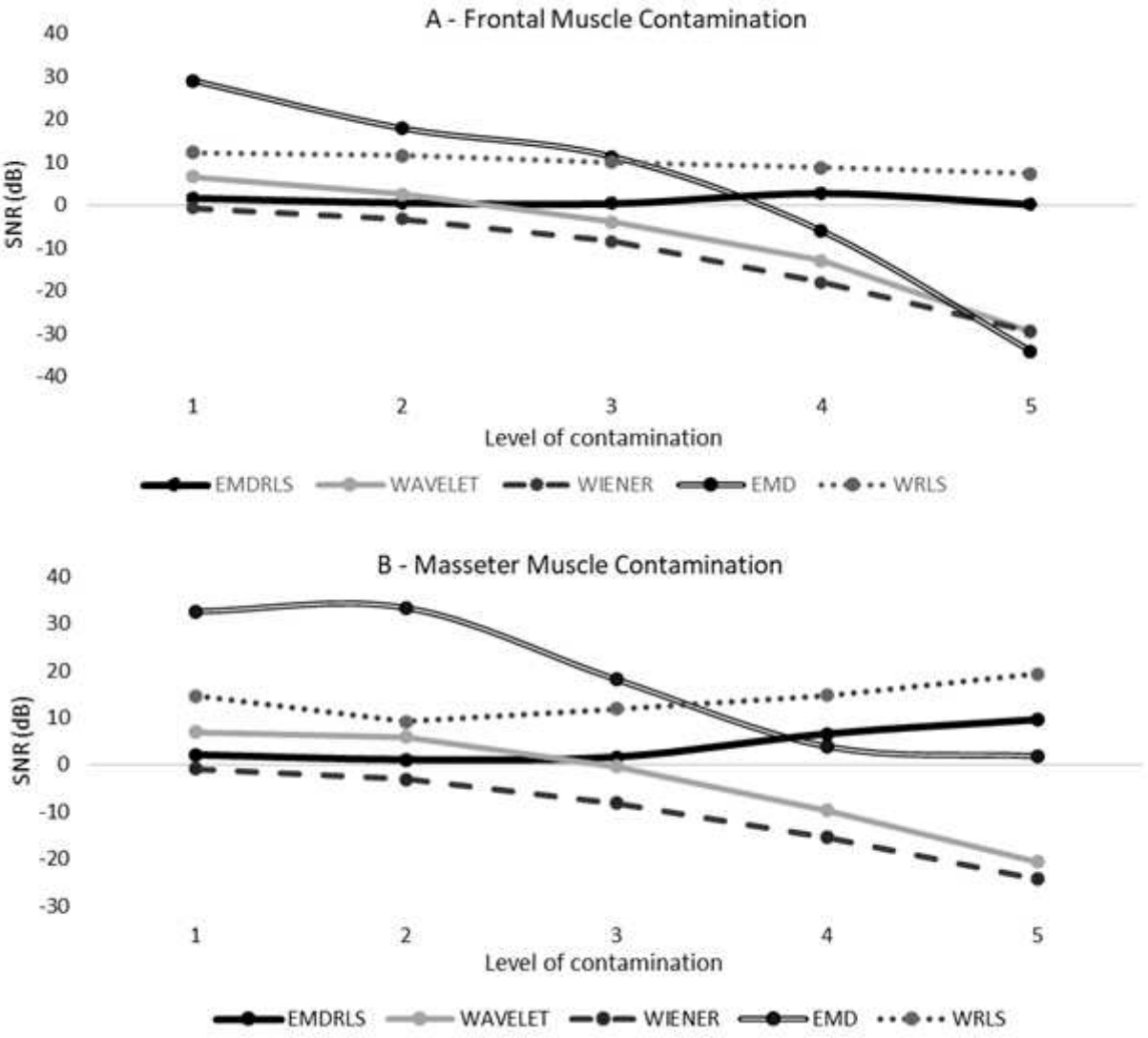

Figure 2

Relationship between the contamination level and the SNR of the filtered signal contaminated by the EMG from the frontal (A) and masseter (B) muscles.

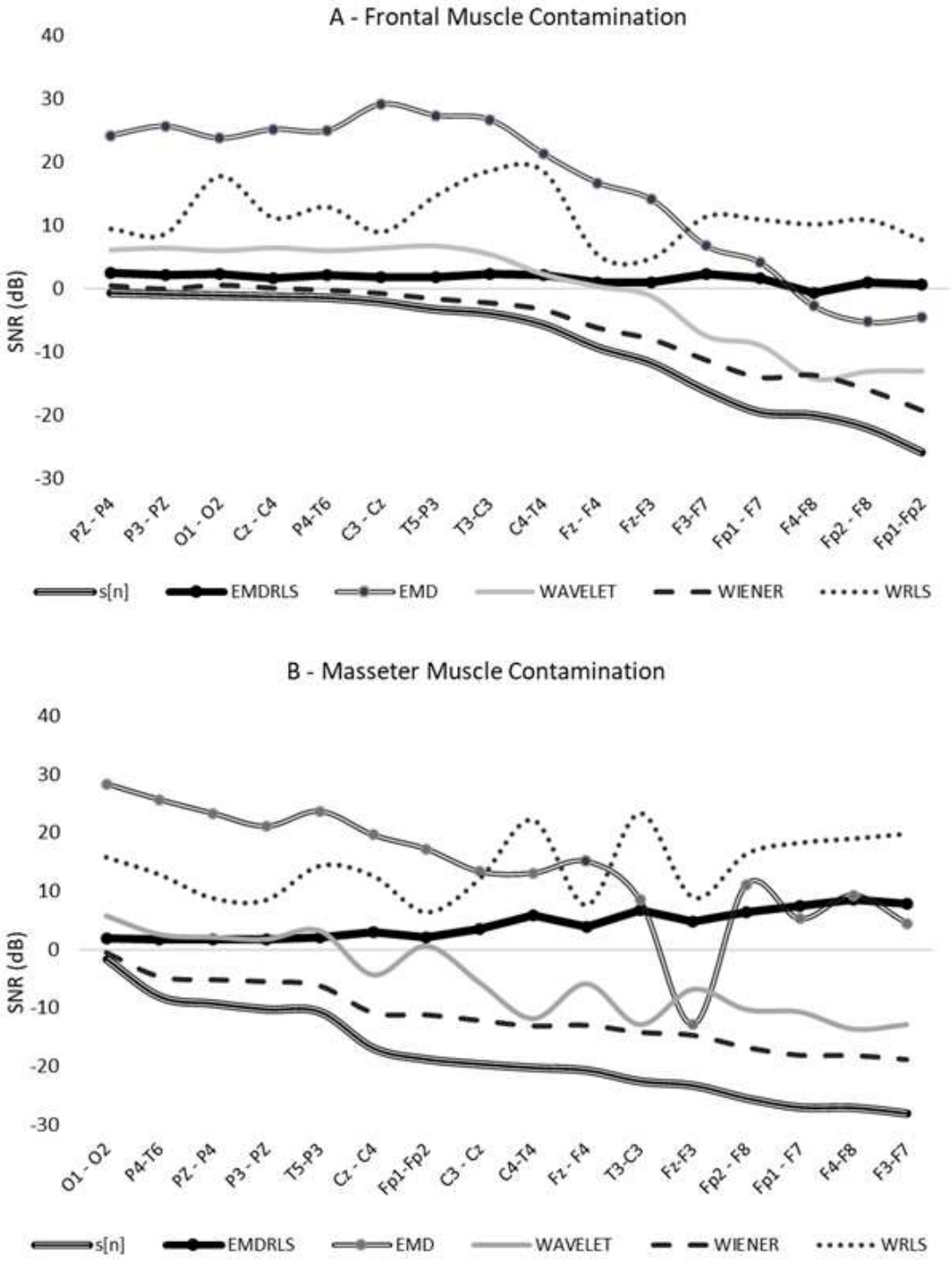

Figure 3

Overall mean SNR of the filtered EMG from the frontal (A) and masseter (B) muscles in relation to each EEG channel. The overall mean SNR of the contaminated EEG signal, s[n], is also shown.

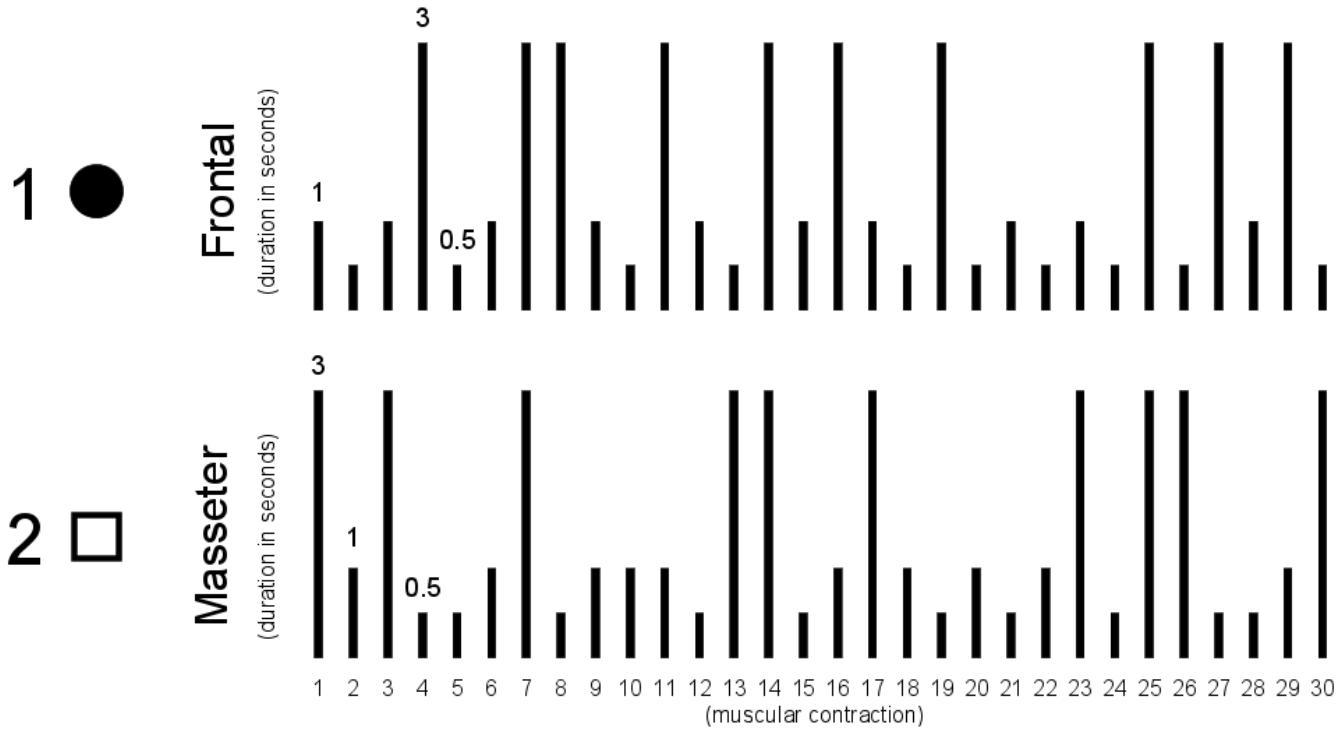

Figure 4

Example of an experiment with random sequences of auditory stimuli for the frontal (1 – circle) and masseter (2 - square) muscles. The vertical bars indicate the duration of the control auditory stimulus. The trial with the masseter muscle (2) starts after the end of the trial with the frontal muscle (1).

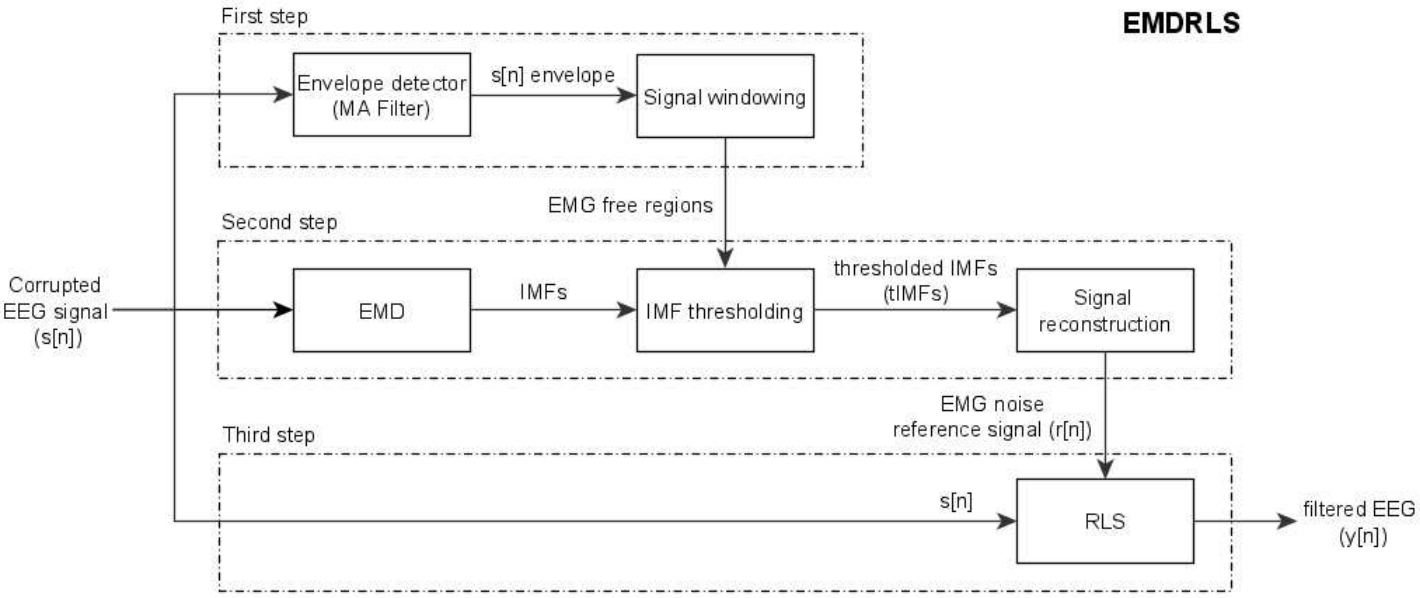

Figure 5

Block diagram of the EMDRLS technique for noise attenuation in EEG signals. First step: Signal regions without EMG are detected. Second step: The input signal s[n] is decomposed into IMFs and then the EMG-free regions are thresholded so that an EMG noise reference signal (r[n]) is generated. Third step: The input signal, s[n], is filtered by an RLS filter with a reference signal (r[n]), resulting in a filtered EEG signal (y[n]).

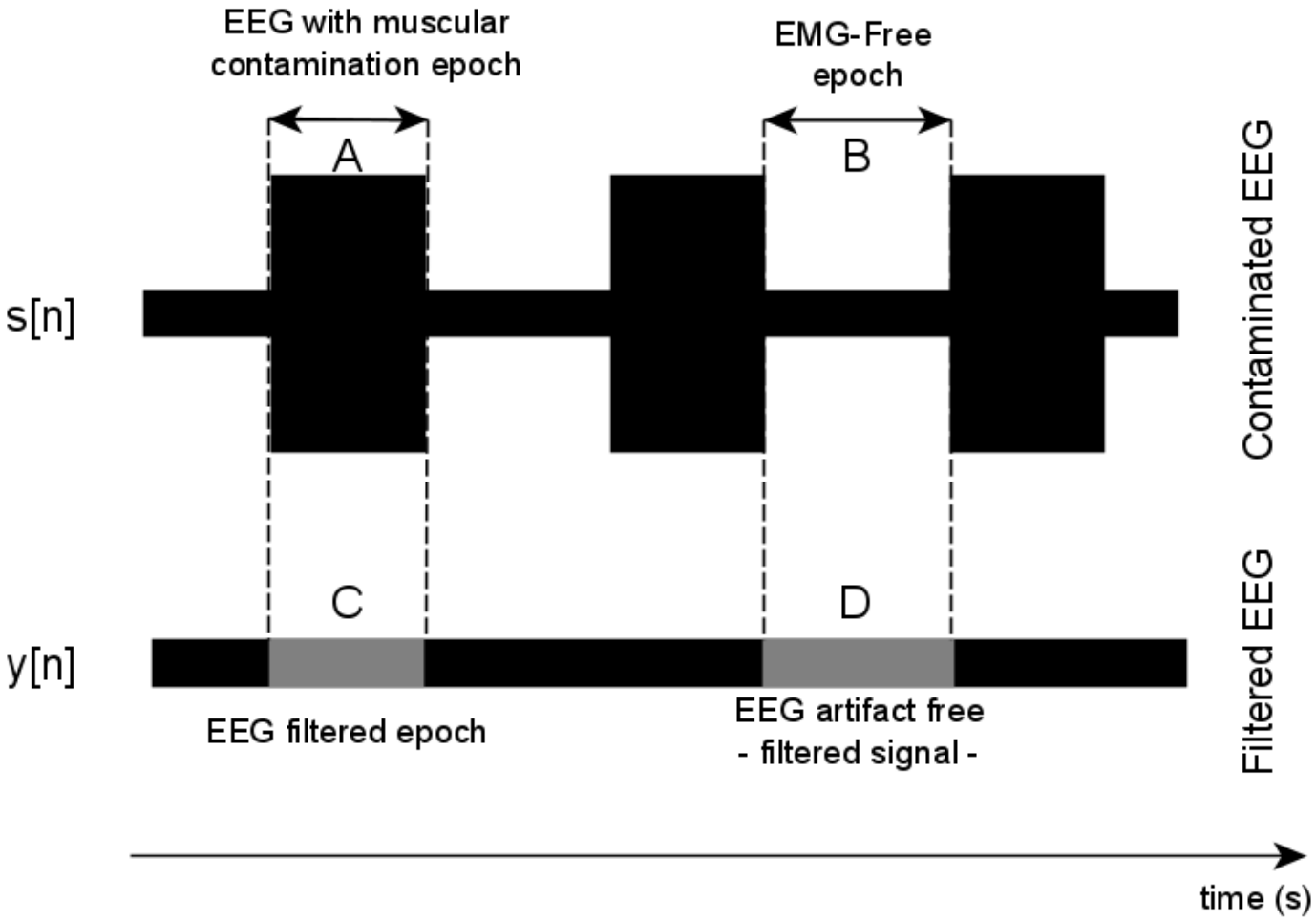

Figure 6

Definition of signal regions (A, B, C and D) for the estimation of the performance metrics. s[n] is the corrupted signal and y[n] is its corresponding filtered version. A is the signal region corrupted by EMG, whereas C is the corresponding filtered signal. B is the EMG-free region and D the corresponding filtered signal.

Supplementary Files

This is a list of supplementary files associated with this preprint. Click to download.

- DatasetFeatures.xlsx